

Modelling and Image Reconstruction Evaluation of a Scintillation Camera with Silicone Photomultiplier

Md Ali Sham Firdaus^{1,2*}, Saripan M. Iqbal³, Muhammad Noor Ahmad Shukri³, Rokhani Fakhru Zaman³, Hashim Suhairul⁴, Xianling Dong⁵

ABSTRACT

Background: Recent research on photon detection has led to the introduction of a silicone photomultiplier (SiPM) that operates at a low voltage and is insensitive to magnetic fields.

Objective: This work aims to model a scintillation camera with a SiPM sensor and to evaluate the camera reconstructed images from gamma ray projection data.

Material and Methods: The type of study in this research is experimental work and analytical. The scintillation camera, modelled from an SiPM sensor array SL4-30035, coupled with a scintillation material Caesium Iodide doped with Thallium (CsI(Tl)), is used in the experimental part. The performance of the camera was evaluated from reconstructed images by a back-projection technique of a radioactive source Caesium-137 (Cs-137).

Results: The experiments conducted with a 1 μ Ci Cs-137 radioactive source have revealed that the bias voltage (V_{bias}) of the SiPM needs to be set to 27.8 V at an operating temperature between 43 °C to 44 °C. The radioactive source has to be placed within a 1 cm distance from the sensor to obtain the optimum projection data. Finally, the back-projection technique for image reconstruction with linear interpolation pre-processing has revealed that the Ram-Lak filter produces a better image contrast ratio compared to others.

Conclusion: This research has successfully modelled a scintillation camera with SiPM that was able to reconstruct images with an 86.4% contrast ratio from gamma ray projection data.

Citation: Sham Firdaus MA, Iqbal SM, Ahmad Shukri MN, Fakhru Zaman R, Suhairul H, Dong X. Modelling and Image Reconstruction Evaluation of a Scintillation Camera with Silicone Photomultiplier. *J Biomed Phys Eng.* 2022;12(2):117-126. doi: 10.31661/jbpe.v0i0.2009-1183.

Keywords

Gamma Cameras; Silicone Photomultiplier (SiPM); Photomultiplier Tubes (PMT); Image Reconstruction; Filter Back-Projection; Radionuclide Imaging; Scintillation Counting

Introduction

Medical imaging techniques from a gamma camera such as Positron Emission Tomography (PET) and Single Photon Emission Computed Tomography (SPECT) have contributed to earlier and more accurate cancer detection. Current gamma cameras are typically built with photomultiplier tubes technology (PMT) for photon detection. However, this conventional technology has been considered costly and space consuming [1]. A typical gamma camera consists of

¹PhD Candidate, Faculty of Engineering, University Putra Malaysia, Serdang, Selangor, Malaysia

²PhD Candidate, Department of Electrical & Electronics, German-Malaysian Institute, Kajang, Selangor, Malaysia

³PhD, Faculty of Engineering, University Putra Malaysia, Serdang, Selangor, Malaysia

⁴PhD, Faculty of Science, University Teknologi Malaysia, Skudai, Johor, Malaysia

⁵PhD, Department of Biomedical Engineering, Chengde Medical University, Chengde, Hebei, China

*Corresponding author: Md Ali Sham Firdaus
Faculty of Engineering,
University Putra Malaysia,
Serdang, Selangor,
Malaysia
E-mail: shamfirdaus@gmi.edu.my

Received: 14 September 2020
Accepted: 12 November 2020

a collimator, scintillation material and a PMT on the back end of the device [2-5]. Common scintillation materials used in SPECT include Sodium Iodide (NaI) and Caesium Iodide (CsI), while common radio tracers include the Technetium (^{99m}Tc), Gallium (^{67}Ga), and Iodine (^{123}I), among others. In SPECT, these radio tracers are injected in the patient's body, and emit gamma rays. The gamma rays are then scintillated by the gamma camera producing light photons. Subsequently, a gamma camera acts by measuring the amount of incident photons and determines the position of the photons incident [6]. Meanwhile, a collimator assists in ensuring the gamma ray beam aligns between the points of exposure from the patient to the camera surface [7-8].

Recent research on photon detection and the capability of the avalanche photodiode (APD) has resulted in the introduction of the silicone photomultiplier (SiPM), which is a photo detector built with high gain capability and operates at a low voltage [2, 9]. The SiPM comprises diodes with breakdown voltage, operating on a specific amount of photon incidents. Each pixel in the SiPM sensor contains thousands of photodiodes, known as microcells. Hence, there is a possibility of the SiPM sensor to be utilized in determining the amount of photon incidents [10]. Moreover, it is insensitive to magnetic fields [1-2]. With these advantages, it has the potential to replace the conventional PMT in gamma cameras. In short, this research contributes in producing medical imaging devices with an alternative solution. However, further research is needed to be conducted on various elements of the SiPM before this is possible.

Several objectives are specified for this research. The first objective is to model and construct a scintillation camera with a SiPM photo based sensor to acquire gamma ray emission from a Caesium-137 (Cs-137) radioactive element. Several important configurations of the camera must be identified, including the sensor optimum operating temperature, proper

bias voltage (V_{bias}) and optimum operating distance. The second objective of this research is to obtain projection data from a radioactive point source by applying the proper camera configuration. Projection data was taken by rotating the camera towards the radioactive point source. Finally, the last objective of this research is to evaluate the scintillation camera performance by reconstructing the images from the projection data. Several different filtering techniques were implemented during the image reconstruction process for evaluation purposes.

Material and Methods

The type of study in this research is experimental work and analytical. This research uses some gamma radiation data acquisition equipment to capture the data projection from a radioactive point source. The research also implements Matlab analytical software for reconstructing images from the projection data. Several experiments and analyses have been conducted in this research to determine the parameters and configurations in acquiring the optimum results from a modelled scintillation camera with a SiPM sensor. These configurations were then applied to an actual experiment in acquiring projection data for image reconstruction.

The first experiment was conducted to determine the optimum operating bias voltage (V_{bias}) for the SiPM sensor. The V_{bias} value was set high enough to allow the sensor to trigger once it detects the low light from the scintillation process, and yet low enough to prevent it from triggering in the absence of a radioactive source.

The second experiment was conducted to determine the optimum operating distance between the radioactive source and the SiPM sensor. A closer distance between them generally increases the sensor readout performance. However, it is more likely that more gamma ray photons pass through the detector without being scintillated.

A scintillation camera was then modelled and constructed based on the outcome of the experiments. Projection data were then extracted from the modelled scintillation camera. Finally, image reconstruction using a back-projection technique was applied to evaluate the performance of the scintillation camera.

Experimental Setup

This research utilizes Caesium-137 (Cs-137) radioactive point source for the experiment. It emits gamma ray photons with energy of 662 keV and also Cs-137 is among the most utilized radioactive sources in the nuclear medical field [11]. The material has an activity of 1 μ Ci, decaying at a rate of 3.7×10^4 disintegrations per second (dps). In addition to this, the material has a longer lifetime of 30 years, and is suitable for long experimental procedures. Furthermore, Cs-137 is widely used in brachytherapy for radiotherapy during the treatment of cancerous patients. In a brachytherapy procedure, the sealed capsule gamma ray radioactive substance is placed in the body to eliminate cancer cells [12].

A radioactive source emits a specific amount of gamma ray photons, depending on several factors, including the half-life of the source, the age of the source, source activity as well as the time exposure. The general relationship can be observed using Equation 1 [13]. According to this equation, the number of emitted gamma ray photons (N) depends on the exposure time t in hours and the radiation activity A . The element T_b is the total branching ratio, with a value of 0.85 for Cs-137 [13].

$$N = T_b \cdot t \cdot A \quad (1)$$

However, since the source was manufactured in 2007, the activity has been slightly reduced. The current activity A can be found by implementing Equation 2 [13]. A_0 represents the initial activity, while t represents the interval after the manufacturing date in years. Lastly, the element τ represents the mean-life of the radioactive source with the same units as the time interval. Currently, the radioactive source for this research disintegrates at a rate of 29×10^3 each second.

$$A = A_0 \cdot e^{-(t/\tau)} \quad (2)$$

This research used the 16 channels SiPM 4×4 detector array SL4-30035 with a peak wavelength absorption of 500 nm, connected to an SIB 1256 interface board. Each sensor pixel dimension is approximately $3 \text{ mm} \times 3 \text{ mm}$ [14]. Measurements of light photons energy scintillated by the scintillation material were collected using the Vertilon IQSP 480 data acquisition system. The experiment setup is shown in Figure 1.

Finally, the experiment for this research utilized the Caesium Iodide doped with Thallium (CsI(Tl)) type of scintillation material. The thickness of this material is 6.35 mm. It is chosen for this experiment as previous research has shown that at a radiation energy level of 662 keV with a scintillation material thickness between 6 mm to 7 mm has the optimal sensitivity and resolution for CsI(Tl) [15].

Furthermore, this scintillation material has a peak wavelength of 550 nm which is closely matching the peak wavelength of the SiPM sensor. The scintillation material CsI(Tl) is considered less hygroscopic compared to the sodium iodide (NaI(Tl)) type of scintillation

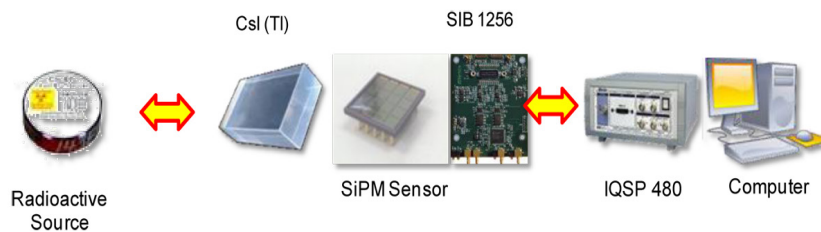


Figure 1: Research experimental setup [13-14].

material. Hence, an aluminum shield case may not be required. Aluminum casing prevents gamma rays from reaching the scintillation material and affecting the energy measurement accuracy during the experiment. A thin aluminum sheet with a thickness of 2.54 mm may potentially prevent up to 98% gamma ray penetration. This was performed by measuring Cs-137 with 1 μ Ci activity using the Spectech ST360 Geiger counter device at a distance of 2 cm for a period of 60 s.

Configuring the SiPM Bias Voltage

The SiPM sensor typically operates at a breakdown voltage (V_{br}) that is slightly higher than the one specified. It is critical to determine the correct V_{bias} of the sensor to prevent the false triggering of the SiPM microcells. Furthermore, it is also important to identify the proper stabilized temperature of the sensor, as the V_{br} value will be affected based on different operating temperatures of the sensor [16].

An experiment was conducted to determine the relationship between the SiPM sensor surface temperature and its operating time. The sensor operates from initial room temperature, and the surface temperature is recorded for every 60 s. This step was repeated until the sensor's temperature is stabilized. Next, the V_{bias} value was determined by operating the SiPM sensor at stabilize temperature. A dark room condition was used throughout the experiment to prevent external lights from reaching

the sensor. Zero calibration was performed on the IQSP480 equipment. In addition to this, a threshold value of the sensor was set to 1×10^{-12} Coulomb (1 pC) to ensure only high energy scintillated gamma rays was captured. The experiment initiates by applying higher V_{bias} and reducing the value until no trigger occurs with the absence of a radioactive source.

Configuring Optimum Operating Distance

The amount of radiation from a radioactive source generally varies under different exposure periods and distances. Determining the optimum distance between the radioactive source and sensor is critical to perform later experiments in modeling a scintillation camera with SiPM. The optimum distance was acquired by finding the most similar photons count between the experimental value and theoretical calculation.

According to this experiment, the point source was directed to channel 6 of the SiPM. The radioactive source Cs-137 was placed at a distance of 1 cm from the SiPM sensor, with the scintillator material in between. Readings were recorded every 60 s at a stabilized operating temperature. The distance was then increased by 1 cm, and the process was repeated until the distance reached 5 cm. The calculation on the triggered microcells was performed on the readings to compare the actual triggered values from the SiPM with the theoretical values. Figure 2 depicts the experimental setup.

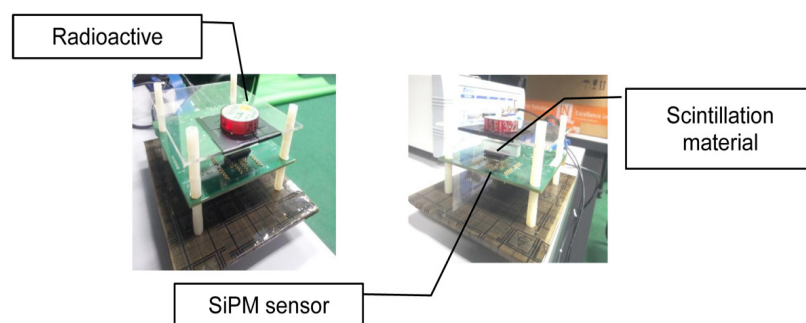


Figure 2: Positioning of radioactive source.

Projection with Scintillation Camera

Finally, the SiPM sensor was implemented in the research scintillation camera to measure the emitted gamma rays from the radioactive source using the parameter acquired from the previous experiment. The optimum bias voltage was applied at the optimum operating temperature of the sensor at an optimum distance. The sensor was rotated on a 360° angle across the radioactive source. The results of the experiment, which are the projection data, were utilized to reconstruct images by applying back-projection method using the Matlab software. Readings were taken across channel 5 to channel 8 of the SiPM sensor. The reconstructed images carried out after several filtering techniques were evaluated.

Results

Scintillation Camera Configuration

From the first experiment, it is found that the SiPM sensor surface temperature will rise from the start of the operation, until it reaches a stable temperature reading. Rapid changes in temperature were encountered during the initial operation time. In addition to this, the surface sensor temperature stabilized after approximately 1,080 s (18 min) at values between 43.0 °C to 43.9 °C. The plotted surface temperature is as shown in Figure 3. Hence, further analysis was conducted at this particular temperature.

Based on the results from the first experiment, the sensor triggers even with the absence of a radioactive source at a bias voltage 28.0 V. Upon reduction of the bias voltage, lesser triggering occurs during a period of 60 s. The optimum operating bias voltage for the sensor is found to be 27.8 V. This value prevents any triggering of the SiPM sensor in the absence of a radioactive source. Readings can only be acquired once it is exposed to a gamma radiated source.

For the second experiment, the readings

from the SiPM sensor were taken upon varying distances of the radioactive source. The trigger count reduces with a higher distance between them. At a distance of 1 cm apart, the SiPM will trigger 501 times in a period of 60 s, accumulating a total charge of 593 pC. The rest of the results are shown in Table 1.

The number of triggered microcells in the SiPM sensor can then be determined by applying Equation 3 in calculating N_{fired} [14]. According to the equation, Q is the accumulated charge and G represents the sensor gain value, while q is the electron charge. Analysis can be performed in comparing the amount of gamma ray photons calculated to reach the sensor, with the amount of actual triggered microcells from the SiPM.

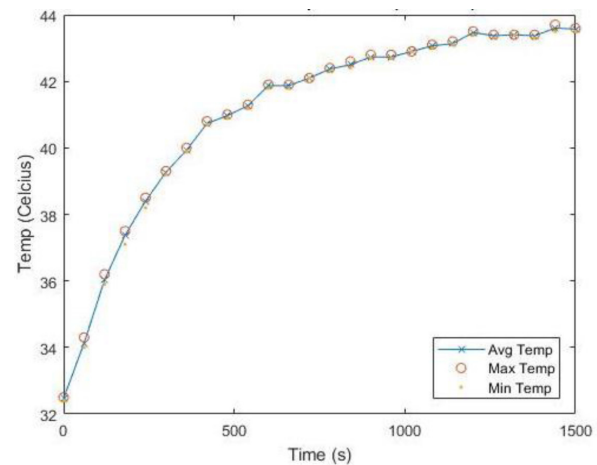


Figure 3: Sensor surface temperature vs operating time.

Table 1: Results of total charge measured with varying distance.

Distance (cm)	Trigger count	Total charge (pC)
1	501	593
2	268	317
3	121	144
4	97	113
5	57	68

$$Q=N_{\text{fired}} \cdot G \cdot q \quad (3)$$

Generally, when the distance between the radioactive source and the sensor is increases, the number of gamma ray photons, reaching the sensor significantly reduces. Equation 4 provides a relationship between the theoretical detector efficiency upon varying distance [14].

$$DE_{\text{ff}}=G \cdot I \cdot M \quad (4)$$

According to the equation, G is the ratio of detector surface area over the sphere area in between the detector and source; I is the fraction of photons from intervening materials; and M is the fraction of Gamma ray photons absorbed by the detector, and significantly depends on the scintillation material thickness. Equation 5 depicts the relationship between scintillation material thickness d and the Gamma ray photons absorbed by the detector M [14]. The attenuation coefficient of the scintillator μ is represented by the value 0.3 cm^{-1} for CsI(Tl) [14]. Typically, for CsI(Tl) material with a thickness of 6.35 mm, the percentage absorption is around 20% [14].

$$M=1- e^{-(\mu \cdot d)} \quad (5)$$

Table 2 indicates the difference between the theoretical calculation and the experimental results after applying Equations 3, 4 and 5.

Firstly, according to the Table 2, the amount of trigger microcells exceeds the desired photons reaching the sensor. This can occur as a single scintillated gamma ray photon might have triggered more than one microcell in a single event. Moreover, scattered photons might also trigger the microcells. Secondly, from the Table 2, the error slightly increases as the distance between the source and the sensor

increased. From Table 2, it is confirmed that the distance of 1 cm apart produces less difference that is better at representing the photon counts from the radioactive source.

Projection Data Image Reconstruction

Next, the SiPM sensor was exposed to the radioactive source at a distance of 1 cm apart for projection data acquisition. Charge measurements were taken at SiPM surface channels 5, 6, 7 and 8 for duration of 10 s. The SiPM sensor was rotated across the radioactive source from 1° until 360° , in 10° increments. A total of 36 different measurements from each angle from the four SiPM channels were recorded. The measurements from each angle were interpolated using the Linear Interpolation technique and fed to the Matlab function for Radon transformation. Data interpolation was basically a mathematical method in constructing new data points from a range of a known discrete set of points [17]. Interpolation in image reconstruction assists in enabling the processing of multi-resolution pixels [18].

An example of the resulted Radon transformation is shown in Figure 4a. All 36 measurements from different angles are summed up to produce the Sinogram image of the projected radioactive source. The sample of the Sinogram image is depicted in Figure 4b.

Discussion

Results from the Sinogram images are analysed in this section to evaluate the performance of the scintillation camera. The filtered

Table 2: Comparing calculated and measured values.

Distance (cm)	Calculated Value (Photons)	Measured value (Triggered microcell)	Difference (%)
1	2147	1542	28.18
2	536	824	53.73
3	238	374	57.14
4	134	295	120.15
5	85	177	108.23

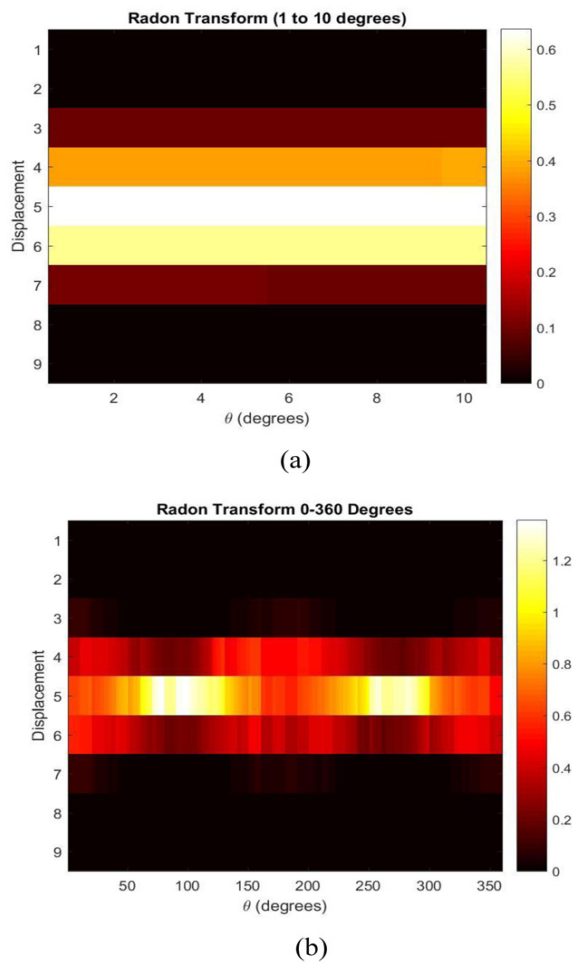


Figure 4: a) Sample of Radon Transformation for angle 1 to 10 degrees, b) Sample of Sinogram image.

back-projection (FBP) technique was applied to each of the Sinogram images to generate the reconstructed image. FBP is a common technique used for analytical reconstruction [19], and offers simplicity, speed, and computational efficiency [20]. In this particular research, several types of filters were applied during image reconstruction such as the Ram-Lak filter and Shepp-Logan filter.

The reconstructed images were evaluated in terms of contrast value, as shown in Table 3. The contrast of an image is basically the ratio between the image highest luminance (L_H) and the lowest luminance (L_L) [21]. For evaluation purposes, the Weber contrast (C_w) equa-

tion was applied to the reconstructed images. The Weber contrast value was determined by applying Equation 6 [21]. The maximum contrast of an image by Weber contrast has a value of 1, while the lowest has a value of 0. The constructed images are as shown in Figures 5a to f.

$$C_w = \frac{L_H - L_L}{L_H} \quad (6)$$

According to the results, the experimental setup was able to scintillate the radioactive source material. Furthermore, the light photons generated were able to trigger the SiPM sensor. Based on the results of the reconstructed images, the SiPM sensor was able to produce better contrast when the filtering technique was applied. During the analysis, the Ram-Lak filter was able to produce a high contrast ratio of approximately 86%. This filtering technique also shows better image and contrast compared to other filtering techniques. This is due to the fact that the Ram-Lak filter introduced by Ramachandran and Lakshminarayanan implements a windowing function to a standard Ramp filter to reduce the noise of higher frequency in the reconstructed images [15].

Conclusion

A model of a scintillation camera using a SiPM sensor was introduced in this research. The experiment in the research uses the SiPM sensor array SL4-30035. This sensor has 16

Table 3: Reconstructed image Contrast Ratio of with various Back-Projection filtering techniques.

Pre-processing done	Applied Filter	Contrast ratio (%)
Linear interpolation	None	60.64
Linear interpolation	Ram-Lak	86.44
Linear interpolation	Shepp-Logan	84.41
Linear interpolation	Cosine	78.68
Linear interpolation	Hanning	75.05
Linear interpolation	Hann	73.06

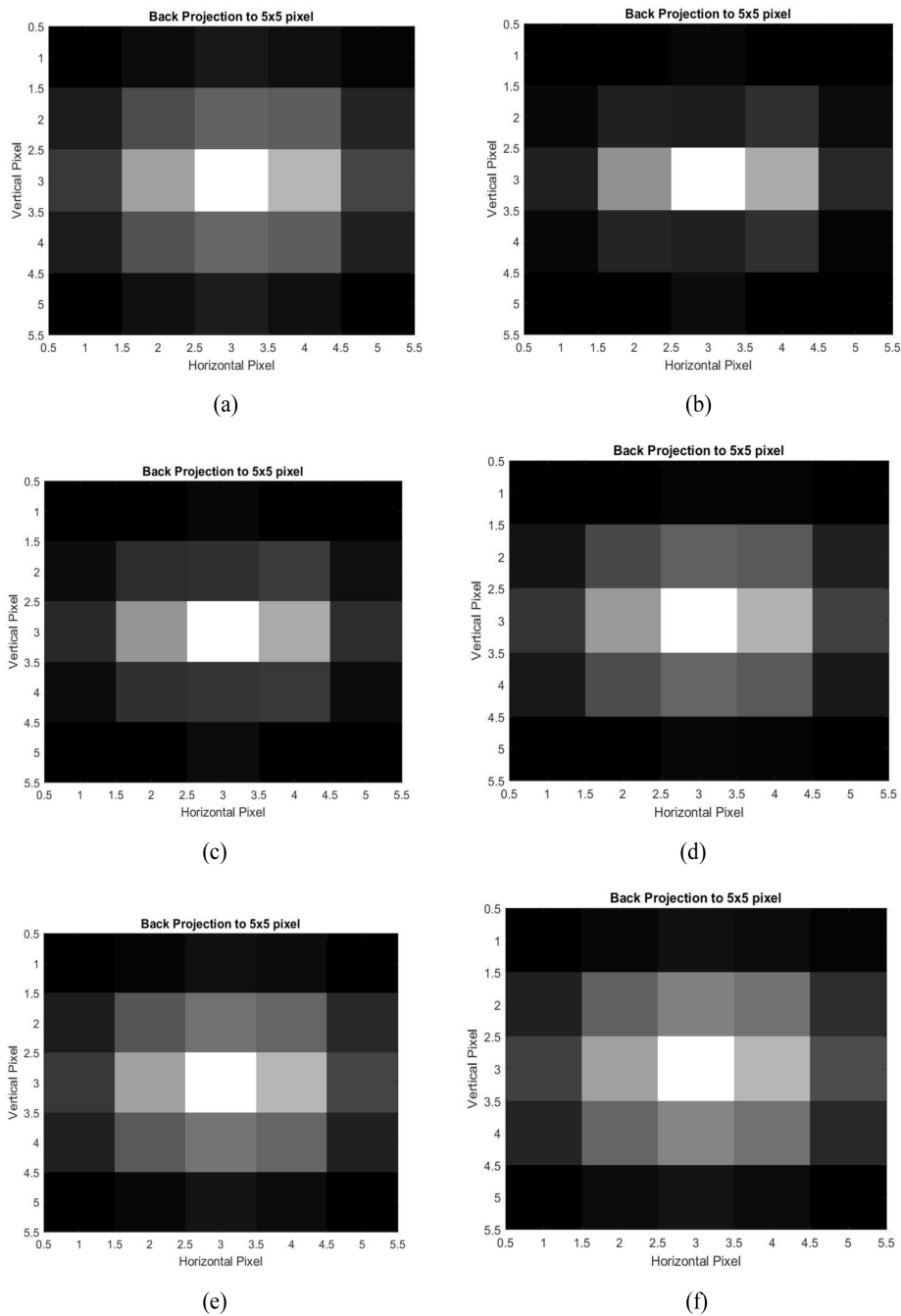


Figure 5: a) Reconstructed image without Filter, b) Reconstructed image with Ram-Lak Filter, c) Reconstructed image with Shepp-Logan Filter, d) Reconstructed image with Cosine Filter, e) Reconstructed image with Hamming Filter, f) Reconstructed image with Hann Filter.

pixels, each with a dimension of approximately $3 \text{ mm} \times 3 \text{ mm}$. The experiment also used the radioactive source Caesium-137 (Cs-137) to emit gamma rays. The experiment was set up using crystal CsI(Tl) as the scintillation material with a thickness of 6.35 mm. Dur-

ing this research, it was found that the surface temperature of the SiPM sensor stabilizes after approximately 18 min of operation. The temperature stabilizes at an approximate temperature value of $43 \text{ }^\circ\text{C}$ to $44 \text{ }^\circ\text{C}$. This is considered the optimum temperature to operate the

sensor. Next, the optimum bias voltage was obtained from the experimental procedure. It is found that a bias voltage of 27.8 V is the optimum bias voltage required to ensure that the sensor will only trigger with the presence of a radioactive source. From the experimental results, a 1 cm distance between the SiPM sensor and the radioactive source produced closely matched measurements with the theoretical values. Hence, it is concluded that a closer distance between the radioactive source and the sensor will produce less error compared to the theoretical values. Therefore, this distance will be used in further experiments with SiPM. This scintillation camera model was then used to acquire a 360° projection measurement of the radioactive source. A full rotation of the sensor towards the source was performed due to the stochastic nature of the gamma emitted radioactive source. The reconstructed images were then produced from the readings by applying different types of filtering techniques. From the reconstructed images, the image using the Ram-Lak filter produced better contrast compared to others. For future research, it is suggested that more image reconstruction interpolation and filtering techniques are applied to evaluate the overall performance of the sensor.

Acknowledgment

This research was guided and supervised by lecturers from University Putra Malaysia, and University Teknologi Malaysia. All authors have no conflict of interest to report. Any suggestions, recommendations and conclusions in these writings are from the authors. This research also acknowledges the contribution from the Fundamental Research Grant Scheme FRGS/2/2014/TK03/UPM/02/3 from the Ministry of Higher Education and Ministry of Science, Technology and Innovation 5450786.

Authors' Contribution

MA. Sham Firdaus conducted the experimental work, data collection, data analysis and drafted the manuscript. H. Suhairul, R. Fakhrul Zaman and

MN. Ahmad Shukri prepared the experimental apparatus. X. Dong assisted in performing the experimental work. SM. Iqbal supervised all the steps of the study. All authors read and approved the initial and final draft of this manuscript.

Ethical Approval

This article does not contain any studies with human participants or animals.

Funding

This research project was funded by University Putra Malaysia Research Grant Scheme FRGS/2/2014/TK03/UPM/02/3 from the Ministry of Higher Education and Ministry of Science, Technology and Innovation (5450786).

Conflict of Interest

None

References

- Otte N. The silicon photomultiplier-a new device for high energy physics, astroparticle physics, industrial and medical applications. International Symposium On Detector Development For Particle, Astroparticle And Synchrotron Radiation Experiments (SNIC 2006); Menlo Park, California: eConf C0604032; 2006.
- Roncali E, Cherry SR. Application of silicon photomultipliers to positron emission tomography. *Ann Biomed Eng.* 2011;**39**(4):1358-77. doi: 10.1007/s10439-011-0266-9. PubMed PMID: 21321792. PubMed PMCID: PMC3069330.
- Roslan RE, Saad WM, Saripan MI, Hashim S, Choong WS. The performance of a wire mesh collimator SPECT camera for different breast volumes in prone position. *Nucl Instrum Methods Phys Res A.* 2010;**619**(1-3):385-7. doi: 10.1016/j.nima.2009.11.005.
- Saripan MI, Petrou M, Wells K. Design of a wire-mesh collimator for gamma cameras. *IEEE Trans Biomed Eng.* 2007;**54**(9):1598-612. doi: 10.1109/TBME.2007.902584. PubMed PMID: 17867352.
- Saripan MI, Saad WH, Hashim S, Mahmud R, Nordin AJ, Mahdi MA. Monte carlo simulation on breast cancer detection using wire mesh collimator gamma camera. *IEEE Trans Nucl Sci.* 2009;**56**(3):1321-4. doi: 10.1109/TNS.2008.2012058.
- Moehrs S, Del Guerra A, Herbert DJ, Mandelkern

- MA. A detector head design for small-animal PET with silicon photomultipliers (SiPM). *Phys Med Biol*. 2006;**51**(5):1113-27. doi: 10.1088/0031-9155/51/5/004. PubMed PMID: 16481681.
7. Dong X, Saad WH, Adnan WA, Hashim S, Hassan NP, Saripan MI. Simulation of intrinsic resolution of scintillation camera in Monte Carlo environment. IEEE International Conference on Signal and Image Processing Applications; Melaka, Malaysia: IEEE; 2013. doi: 10.1109/ICSIPA.2013.6707969.
 8. Ali SM, Xianling D, Noor AM, Rokhani FZ, Hashim S, Saripan MI. Modelling of light photons detection in scintillation camera. IEEE International Conference on Signal and Image Processing Applications; Melaka, Malaysia: IEEE; 2013. doi: 10.1109/ICSIPA.2013.6707970.
 9. Alnafea M, Wells K, Spyrou NM, Saripan MI, Guy M, Hinton P. Preliminary results from a Monte Carlo study of breast tumour imaging with low-energy high-resolution collimator and a modified uniformly-redundant array-coded aperture. *Nucl Instrum Methods Phys Res A*. 2006;**563**(1):146-9. doi: 10.1016/j.nima.2006.01.124.
 10. Peterson TE, Furenlid LR. SPECT detectors: the Anger Camera and beyond. *Phys Med Biol*. 2011;**56**(17):R145-82. doi: 10.1088/0031-9155/56/17/R01. PubMed PMID: 21828904. PubMed PMCID: PMC3178269.
 11. Thoraeus R. Cesium 137 and its gamma radiation in teleradiotherapy. *Acta radiol*. 1961;**55**:385-95. doi: 10.3109/00016926109175133. PubMed PMID: 13776672.
 12. Banahene JO, Darko EO, Awuah B. Low dose rate caesium-137 implant time of intracavitary brachytherapy source of a selected oncology center in Ghana. *Clin Cancer Investig J*. 2015;**4**(2):158-64. doi: 10.4103/2278-0513.150617.
 13. Saint-Gobain Crystals. Efficiency calculations for selected scintillators. Ohio, USA: Saint-Gobain; 2014.
 14. SensL Technologies, LTD. Introduction to SiPM, technical note. Cork, Ireland: Sense Light Corporation; 2017.
 15. Monachesi E, Dezi A, D'Ignazio M, Scalise L, et al. Comparative Evaluation of Cesium Iodide Scintillators Coupled to a Silicon Photomultiplier (SiPM): Effect of Thickness and Doping on the scintillators. *J Phys Conf Ser*. 2017;**931**(012013):1-5. doi: 10.1088/1742-6596/931/1/012013.
 16. SensL Technologies, LTD. ArraySL-4 Scalable silicon photomultiplier array data sheet. Cork, Ireland: Sense Light Corporation; 2011.
 17. Information Resources Management Association. Medical Imaging: Concepts, Methodologies, Tools, and Applications. USA: IGI Global; 2016.
 18. Leng J, Xu G, Zhang Y. Medical image interpolation based on multi-resolution registration. *Comput Math Appl*. 2013;**66**(1):1-18. doi: 10.1016/j.camwa.2013.04.026.
 19. Willeminck MJ, Noël PB. The evolution of image reconstruction for CT-from filtered back projection to artificial intelligence. *Eur Radiol*. 2019;**29**(5):2185-95. doi: 10.1007/s00330-018-5810-7. PubMed PMID: 30377791. PubMed PMCID: PMC6443602.
 20. Lyra M, Ploussi A. Filtering in SPECT image reconstruction. *Int J Biomed Imaging*. 2011;**2011**(10):1-14. doi: 10.1155/2011/693795. PubMed PMID: 21760768. PubMed PMCID: PMC3132528.
 21. Ortiz Jaramillo B, Kumcu A, Platasa L, Philips W. Content-aware contrast ratio measure for images. *Signal Process Image Commun*. 2018;**62**:51-63. doi: 10.1016/j.image.2017.12.007.